The American Journal of Pathology, Vol. 175, No. 6, December 2009

DOI: 10.2353/ajpath.2009.080954

Cell Injury, Repair, Aging and Apoptosis

Gene Expression Profiling of Pulmonary Fibrosis Identifies Twist1 as an Antiapoptotic Molecular "Rectifier" of Growth Factor Signaling

Robert S. Bridges,* Daniel Kass,† Katrina Loh,† Carlota Glackin,‡ Alain C. Borczuk,§ and Steven Greenberg*†

From the Department of Pharmacology, the Division of Pulmonary, Allergy, and Critical Care Medicine,† Department of Medicine, and the Department of Pathology and Cell Biology,§ Columbia University College of Physicians and Surgeons, New York, New York; and the Division of Molecular Medicine,‡ Beckman Research Institute, City of Hope, Duarte, California*

Idiopathic pulmonary fibrosis (IPF) is a progressive and typically fatal lung disease. To gain insight into IPF pathogenesis, we performed gene expression profiling of IPF lungs. Twist1, a basic helix-loop-helix protein, was found among the most consistently and highly up-regulated genes and was expressed in nuclei of type II epithelial cells, macrophages, and fibroblasts in IPF lungs. We studied the function of Twist1 in fibroblasts further, because they are the major effector cells in this disease and persist despite an ambient proapoptotic environment. Twist1 was induced by the profibrotic growth factors (GFs) basic fibroblast growth factor, platelet-derived growth factor, and epidermal growth factor in primary rat lung fibroblasts (RLFs). Suppression of Twist1 expression resulted in decreased RLF accumulation due to increased apoptosis, whereas Twist1 overexpression protected RLFs against several apoptotic stimuli. Addition of platelet-derived growth factor in combination with other GFs led to an increase in proliferation. When Twist1 was depleted, GFs continued to act as mitogens but caused a marked increase in cell death. The increase in apoptosis under basal or growth factor-stimulated conditions was partly mediated by up-regulation of the proapoptotic Bcl-2 family members, Bim and PUMA. These findings indicate that Twist1 promotes survival and accumulation of fibroblasts by shaping their responsiveness to growth factor stimulation. We propose that Twist1 represents one of the factors that promotes pathogenic accumulation of fibroblasts in fibrotic lung disease. ***(Am J Pathol 2009, 175:2351–2361; DOI: 10.2353/ajpath.2009.080954)***

Idiopathic pulmonary fibrosis (IPF) is a chronic, progressive, and typically fatal lung disease characterized by excess deposition of extracellular matrix proteins. Fibroblasts accumulate in IPF lungs and are viewed as a major effector cell type in the disease, because they are a principal source of extracellular matrix proteins that contribute to irreversible scarring (reviewed in Refs. 1 and 2). The source of fibroblasts in IPF is unclear but likely includes a combination of recruitment of circulating fibroblast precursors,[3–5] transdifferentiation of epithelial or endothelial cells into fibroblasts (e.g., epithelial-mesenchymal transformation; EMT),[6,7] and proliferation of resident lung fibroblasts.[8,9] Regardless of their proximate source, fibroblasts in IPF lungs accumulate despite the presence of a hostile, proapoptotic environment. Because these cells exhibit little evidence of apoptosis,[10] this suggests that they possess highly effective mechanisms to evade apoptotic stimuli.

To identify potential mediators of fibroblast accumulation and survival in IPF, we performed gene expression profiling of IPF lungs. Our analysis revealed Twist1 as the most highly up-regulated transcription factor in diseased lungs. Twist1, which is a member of a large family of basic helix-loop-helix proteins, has been implicated in bone and cartilage development,[11,12] regulation of inflammation,[13,14] tumor progression and metastasis,[15–17] and resistance of tumor cells to apoptosis induced by chemotherapeutic agents.[16,18] Thus, we reasoned that Twist1 may play an analogous role in primary lung fibroblasts subjected to the harsh

Supported by 1K08HL083085, 2P30ES009089, the Stony Wold-Herbert Fund of New York, and the Janet and Tony Goldman Fund for Innovative Lung Research.

Accepted for publication August 25, 2009.

Supplemental material for this article can be found on *http://ajp.amjpathol.org*.

Address reprint requests to Steven Greenberg, M.D., Merck Research Laboratories, 126 East Lincoln Avenue, Rahway, NJ 07065-0900. E-mail: steven.greenberg@merck.com.

proapoptotic conditions that characterize IPF lungs. In this study, we tested whether Twist1 expression affects proliferation, survival, or both of primary lung fibroblasts exposed to various GFs and apoptotic stimuli present in IPF lungs.

Materials and Methods

Reagents

Dulbecco's modified Eagle's medium (DMEM) and fetal bovine serum (FBS) were from Invitrogen (Carlsbad, CA). Rat platelet-derived growth factor (PDGF)-BB and human epidermal growth factor (EGF) were from R&D Systems (Minneapolis, MN). Human basic fibroblast growth factor (bFGF) and human soluble Fas ligand were from PeproTech (Rocky Hill, NJ). 4-Hydroxynonenal was from Cayman Chemicals (Ann Arbor, MI). Insulin-selenium-transferrin supplement, human endothelin-1, and thapsigargin were from Sigma-Aldrich (St. Louis, MO). Protein S from human plasma was from Calbiochem/EMD Biosciences (Darmstadt, Germany). Antibodies against Bim (numbers 2819 and 2933), PUMA (number 4976), Bak (number 3814S), Bad (number 9292), and Bik (number 4592) were from Cell Signaling Technology (Beverley, MA). Antibodies against Bik (E-20), actin (I-19), Bcl-Xl (H5); Mcl-1 (S-19), Bax (N-20), and Bcl-2 (C-21), were from Santa Cruz Biotechnology (Santa Cruz, CA). Monoclonal Ab against 5-bromo-2′-deoxyuridine (BrdU) (clone BMC9318) was from Roche Diagnostics (Indianapolis, IN). Monoclonal Ab against 4-hydroxy-2-nonenal (4-HNE) (clone N45.1) was from the Japan Institute for the Control of Aging (Shizuoka, Japan). Monoclonal Ab against FLAG (clone M2) was from Sigma-Aldrich. Monoclonal Ab against tubulin (clone E7) was from the Developmental Hybridoma Bank (University of Iowa, Iowa City, IA). We generated antibodies against Twist1 using the following peptide from rat Twist1: DSLSNSEEEPDRQQPASGKRGARKR. Peptide synthesis, conjugation to keyhole limpet hemocyanin, injection into rabbits, and serum collection were performed by GenScript (Piscataway, NJ). We affinity-purified IgG using a peptide affinity column. Horseradish peroxidase-, fluorescein isothiocyanate-, rhodamine-, and Cy5-conjugated $F(ab')_2$ fragments of donkey anti-goat, -rabbit, and -mouse IgG were from Jackson ImmunoResearch Laboratories (West Grove, PA). Alexa Fluor 488- or 594-conjugated anti-mouse, anti-rabbit, or anti-goat IgG, and 4′,6-diamidino-2-phenylindole diacetate (DAPI) were from Molecular Probes/Invitrogen (Carlsbad, CA). A plasmid-encoding Twist1-FLAG and vector control were a gift from E. Olson (University of Texas Southwestern Medical Center, Dallas, TX). The PUMA-FLAG construct was from the laboratory of Dr. L. Greene (Columbia Medical Center, New York, NY). All short hairpin RNA (shRNA) constructs were cloned into the pSIREN-RetroQ-zsGreen vector (BD Clontech, Mountain View, CA). The shLUC negative control (from BD Clontech, sequence not provided) and shBim pSIREN (target sequence: 5′-GACAGAGAAGGTGGACAATTG-3′) were also from Dr. L. Greene. The target sequence for PUMA was 5′-CGGAGACAAGAAGAGCAACAT-3′.

Gene Expression Profiling

Total RNA extraction: mRNA samples were taken from surgical lung biopsies from 7 normal and 10 IPF samples, with 3 of the IPF samples from microdissected fibroblastic foci (Table 1). For extraction from whole-lung biopsies, tissue sections were homogenized with a rotor-stator homogenizer before purification. For microdissected samples, serial 8 μmol/L sections of frozen tissue were obtained. The first section was stained with H&E to ascertain areas containing fibroblastic foci, and foci from the remainder were stained with eosin, microdissected with a 20-gauge needle and collected in a pipette tip under vacuum. Total RNA was extracted using RNEasy columns (Qiagen, Valencia, CA), quantitated by spectrophotometry, and agarose gel electrophoresis was performed to confirm lack of RNA degradation.

Table 1. Demographic Data of Patients Used in This Study

Sample no.	Classification	Age (yr)/Sex	Specimen type	Tissue diagnosis
1	Normal	70/F	Lobectomy	Adenocarcinoma
2	Normal	81/M	Lobectomy	NSCLC
3	Normal	65/M	Lobectomy	SCC
4	Normal	69/F	Lobectomy	NSCLC
5	Normal	66/F	Lobectomy	Adenocarcinoma
6	Normal	66/F	Lobectomy	Adenocarcinoma
7	Normal	70/F	Lobectomy	NSCLC
8	IPF	53/F	Explant	IPF
9	IPF	59/F	Explant	IPF
10	IPF	68/M	Biopsy	IPF
11	IPF	53/F	Explant	IPF
12	IPF	59/F	Explant	IPF
13	IPF	68/M	Biopsy	IPF
14	IPF	43/F	Explant	IPF
15	IPF	61/M	Biopsy	IPF
16	IPF	58/M	Biopsy	IPF
17	IPF	61/F	Explant	IPF

Samples 1 to 7 are from pathologically normal tissue taken from surgical lobectomies of lung cancer patients. Samples 8 to 10 are derived from microdissected fibroblastic foci taken from samples 11 to 13. Samples 11 to 17 are homogenates of grossly abnormal lung, selected for abundance of fibroblastic foci. NSLC, non-small cell lung carcinoma; SCC, Small cell lung carcinoma.

Probe Preparation and Hybridization

Two micrograms of total RNA was reverse transcribed using the Superscript Choice reverse transcriptase and a T7 oligo dT primer (Invitrogen). After second strand synthesis, cDNA was assessed for quality by agarose gel electrophoresis. Biotinylated probe RNA was generated using the Enzo high efficiency bioarray kit (Enzo Biochem, New York, NY). After chemical fragmentation at 95°C, 15 μg of labeled RNA was used for hybridization on a U95Av2 chip (Affymetrix, Santa Clara, CA). Hybridization and array scanning were performed by the Columbia Genome Center. The quality of the microarray was assessed by visual inspection of the .cel images by examining the scaling factor, and by noting a consistent number of present, absent, and marginal calls across comparable samples. The 3′ to 5′ ratio of glyceraldehyde-3-phosphate dehydrogenase was used as an additional quality control parameter, with a goal of 1 to 3 for samples to be acceptable.

Data Analysis

The array was first analyzed using the Affymetrix MAS 5.0 software. An average intensity value was calculated for each probe cell, excluding bordering pixels and using a 75% percentile value of the remaining pixels. Once background and noise values were subtracted, the image was stored in .cel files. Positive and negative calls were generated for each probe pair (perfect match and mismatch), and then a present, absent, or marginal call was assigned to the entire probe set. These calls, as well as raw intensity values, were recorded in a spreadsheet and imported into GeneSpring 5.0 software (Agilent Technologies, Santa Clara, CA). After normalization, data were globally filtered to exclude genes that showed low expression across all samples, and then a second global filter was used for genes that showed excessive variability across the samples. This 7814 gene list was used for unsupervised clustering. In addition, a supervised approach was used to determine whether sets of genes were statistically associated with IPF. A permutation test and neighborhood analysis was performed using Cluster and TreeView software (http://rana.lbl.gov/EisenSoftware.htm). The significance score for each gene was assessed by nearest neighbor *t*-test analysis after randomly permuting the class assignments 1000 times. This analysis determined that ~10% of the 7814 genes had statistically significant ($P < 0.05$) changes in expression in IPF.

Tissue Immunohistochemistry

For immunohistochemistry, lungs were fixed in 10% formaldehyde and embedded in paraffin. Five-micrometer sections were cut and mounted on positively charged glass slides. Sections were deparaffinized with xylene, followed by rehydration with a graded ethanol series and stained with the indicated antibodies. All antigens were developed with the Vectastain ABC Universal kit and diaminobenzidine (Vector Laboratories, Burlingame, CA). Sections were counterstained with Harris' hematoxylin (Sigma-Aldrich), dehydrated through graded alcohol series, and mounted with Permount (Fisher, Fairlawn, NJ). Sections were visualized on an Olympus CHS microscope (Olympus, Tokyo, Japan).

Isolation, Culture, and Transfection of Rat Lung Fibroblasts

Female Sprague-Dawley rats (150–250 g) were purchased from Harlan (Indianapolis, IN). Rats were sacrificed with Euthanasia-5 solution. The lungs were perfused with cold PBS, and the parenchyma were excised. Large airways were carefully removed, and lungs were minced and digested in a 1.25% trypsinizing solution for 90 minutes. After passage through sterile gauze, the cell suspension was pelleted and the cells were maintained in DMEM supplemented with 10% FBS, 5 ng/ml PDGF-BB, 10 ng/ml EGF and insulin-transferrin-selenite liquid supplement. The RLFs were incubated in 5% CO_2 at 37°C, and used for experiments during passages 2–6.

Small Interfering RNA

RLFs were plated in DMEM with 10% FBS and immediately transfected with 37.5 ng of RNA oligomers and 3 μl of Hiperfect (Qiagen) according to the fast-forward protocol in the manufacturer's instructions. One day after initial transfection, the cells were washed once with DMEM and placed in DMEM with the indicated serum concentrations, and fresh transfection complexes were added. Target sequences for small interfering (si)RNA complexes were as follows: nontargeting control small interfering RNA (siRNA), 5′-ACACGAGGUACGCCGACAA-3′; Twist-siRNA1, 5′-ACGAGGAGCUGCAGACACA-3′ (designed and synthesized by Dharmacon); and Twist-siRNA2, 5′-ACUCCAAGAUGGCAAGCUG-3′ (synthesized by Qiagen).

Plasmid Transfection

RLFs were plated 1 day before transfection in DMEM and 10% FBS. The next day, transfection complexes containing 0.5 μg of plasmid and 1.5 μl of Lipofectamine LTX (Invitrogen) were added to the cells according to the manufacturer's instructions. After 5 hours, the cells were washed and incubated overnight in DMEM and 10% FBS. For Twist1 overexpression experiments, cells were incubated overnight in DMEM and 0.5% FBS before adding the indicated reagents. Where applicable, plasmids were cotransfected with an enhanced green fluorescent protein (GFP) expression vector to visualize transfected cells. We routinely observed >90% cotransfection efficiency. We determined that cotransfection of multiple siRNA oligomers was inefficient. Instead, we used a combination of plasmid-based shRNA and siRNA oligomers to suppress multiple genes. For experiments with dual transfection of plasmid shRNA and siRNA oligomers, we plated 1.5×10^5 RLFs in 6-well plates and performed shRNA transfection 1 day later with Lipofectamine LTX as described above. The cells were incubated further at

37°C for 18–24 hours, trypsinized, replated, and transfected with siRNA oligomers as described above.

Quantitative Real-Time PCR

mRNA was isolated from human surgical lung biopsies or whole mouse lungs by tissue disruption with a rotor-stator homogenizer followed by purification with the RNEasy mini kit (Qiagen). For experiments with RLFs, cells were plated at 1.2×10^4 in duplicate or triplicate in 24-well plates and treated as described. mRNA was reverse-transcribed to cDNA using the Quantitect RT kit (Qiagen) and qPCR was performed using the *POWER* SYBR Green PCR Master Mix (Applied Biosystems) and a LightCycler 2.0 RealTime PCR System (Roche Diagnostics). Copies of cDNA were normalized to expression of housekeeping genes glyceraldehyde-3-phosphate dehydrogenase or peptidyl-prolyl isomerase (PPIA). We confirmed specific amplification of the target genes by analyzing dissociation curves and agarose gel electrophoresis following PCR. Primers had the following sequences: human Twist1, forward, 5′-CGGGTCATGGCTAACGTG-3′, and reverse, 5′-CAGCTTGCCATCTTGGAGTC-3′[17]; rat Twist1, forward, 5′-CGGACAAGCTGAGCAAGATT-3′, and reverse, 5′-CCTTCTCTGGAAACAATGAC-3′; and glyceraldehyde-3-phosphate dehydrogenase, forward, 5′-GACCCCTTCATTGACCTCAAC-3′, and reverse, 5′-CTTCTCCATGGTGGTGAAGA-3′. Primers for Bad, Bid1, Bid3 (Hrk), Bik, Bim, BMF, NOXA, PPIA, and PUMA were Quantitect primers from Qiagen (sequences not provided).

Cell-Based Fluorescence Microscopy, Cell Viability, and Proliferation Analysis

For immunofluorescence, cells were fixed in 3.7% formaldehyde for 5 minutes, followed by permeabilization in 0.2% Triton X-100. Cells were incubated with indicated primary antibody for 30 minutes at room temperature or overnight at 4°C in a humid chamber, washed, and incubated with a fluorophore-conjugated secondary antibody for 30 minutes at room temperature. Following mounting, cells were examined using a Nikon Eclipse TE200-inverted fluorescence microscope equipped with a ×60 Plan Apochromat objective (NA 1.4) and an Orca-S100 Hamamatsu CCD camera. Imaging was performed using MetaMorph software. Quantitation of Twist1 and Bim expression of unprocessed images was performed by microspectrofluorimetry. Fluorescence intensity associated with Twist1 immunoreactivity was determined by calculating average raw pixel intensity of a circular region completely within the nucleus and corrected for background fluorescence of each field, as well as nonspecific IgG staining measured with nonimmune rabbit IgG. RLFs were cotransfected with enhanced GFP and Twist-FLAG or control. Bim is localized to mitochondria and stains in a perinuclear distribution. Fluorescent intensity associated with Bim immunoreactivity was determined in all GFP^+ cells per coverslip by calculating average raw pixel intensity in a circular region completely within this perinuclear area of staining. All comparison images were exposed for the same amount of time. For viability experiments, cells were fixed and stained with DAPI without permeabilizing. Viability was assessed by examining up to 200 GFP-positive cells per replicate for classical markers of apoptosis, including nuclear condensation and morphological changes. To analyze proliferation by BrdU incorporation, RLFs were treated as described and incubated with 10 μmol/L BrdU for the last 12 to 18 hours before fixation. After fixation and permeabilization, the cells were incubated in DNase buffer (100 U/ml DNase, 1 mmol/L Ca^{2+}, and 1 mmol/L Mg^{2+} in PBS) for 45 minutes at 37°C in a humid chamber and then stained with an anti-BrdU mAb. At least 200 cells per replicate in two to three independent experiments were assessed for BrdU incorporation.

Fluorescence-Based Cell Counting and Caspase-3 Assays

To facilitate counting cells, cells were fixed in 3.7% formaldehyde, permeabilized in 0.2% Triton X-100, and stained with the DNA-sensitive dye Sybr green I (Invitrogen). Sybr green fluorescence was quantitated with a plate-reading spectrofluorimeter. Pilot experiments indicated that fluorescence intensity correlated with RLF cell counts in a hemacytometer. All data represent fold changes in cell number following background subtraction. Assays for active caspase-3 were done with the EnzChek Caspase-3 Assay Kit number 2 (Invitrogen) based on the caspase-3 substrate Z-DEVD conjugated to rhodamine 110. RLFs were plated at 0.2 to 0.5×10^4 cells per well in triplicate in 48-well plates. At the indicated time points, all but 50 μl of culture media were removed, and cells were lysed by adding 2.5 μl of 20× lysis buffer to the remaining media and one cycle of freezing and thawing. We then added samples to 2× caspase-3 assay buffer in 96-well plates, incubated the reaction 24 hours at room temperature in the dark, and measured fluorescence intensity on a plate-reading spectrofluorimeter. We confirmed that all fluorescence was specific to caspase-3 by including the specific inhibitor Ac-DEVD-CHO in some samples. After subtracting background, caspase-3 activity was normalized to cell number.

Immunoblotting

For immunoblotting, RLFs were plated at 1.5×10^5 each in three wells of 6-well plates/condition and treated as described previously. At the indicated times, cells were lifted for 5 minutes in trypsin, neutralized in 0.5% FBS, and pelleted at $400 \times g$ for 5 minutes. Cells were lysed in radioimmunoprecipitation assay buffer (150 mmol/L sodium chloride, 0.5% IPEGAL CA-630, 0.5% sodium deoxycholate, 0.05% SDS, 1 mmol/L EDTA, 50 mmol/L sodium fluoride, 1 mmol/L phenylmethylsulfonylfluoride, 10 μg/ml leupeptin, 10 μg/ml aprotinin, and 50 mmol/L Tris-HCl (pH 7.4)) at 4°C for 10 minutes, followed by sonication using a tip-probe sonicator and centrifugation at $13{,}000 \times g$ for 5 minutes to remove insoluble debris. Loading onto SDS-PAGE gels was normalized using the detergent compatible protein assay (Bio-Rad, Hercules,

Table 2. Thirty Most Significantly Up-Regulated Genes in IPF Samples

Affymetrix ID	Gene symbol	Gene name	Entrez gene ID	Fold increase
32249_at	*CFHR1*	Complement factor H-related 1	3078	4.1
40328_at	*Twist1*	Twist homolog (acrocephalosyndactyly 3; Saethre-Chotzen syndrome)	7291	5.5
1396_at	*IGFBP5*	Insulin-like growth factor-binding protein 5	3488	3.0
38722_at	*COL6A1*	Collagen, type VI, α1	1291	2.0
38111_at	*VCAN*	Chondroitin sulfate proteoglycan 2 (versican)	1462	3.9
38650_at	*IGFBP5*	Insulin-like growth factor-binding protein 5	3488	2.9
32306_g_at	*COL1A2*	Collagen, type I, α2	1278	4.3
35740_at	*EMILIN1*	Elastin microfibril interface located protein	11117	2.7
32488_at	*COL3A1*	Collagen, type III, α1	1281	4.2
39542_at	*ENC1*	Ectodermal-neural cortex (with BTB-like domain)	8507	2.0
38112_g_at	*VCAN*	Chondroitin sulfate proteoglycan 2 (versican)	1462	4.4
40161_at	*COMP*	Cartilage oligomeric matrix protein	1311	4.4
1767_s_at	*TGFB3*	Transforming growth factor, β3	7043	2.6
34802_at	*COL6A2*	Collagen, type VI, α2	1292	2.1
38422_s_at	*FHL2*	Four and a half LIM domains 2	2274	3.6
36950_at	*TMED9*	Transmembrane emp24 protein transport domain containing 9	54732	1.9
41139_at	*MAGED1*	Melanoma antigen, family D, 1	9500	1.8
36990_at	*UCHL1*	Ubiquitin carboxyl-terminal esterase L1 (ubiquitin thiolesterase) (PARK)	7345	8.2
39395_at	*THY1*	Thy-1 cell surface antigen	7070	4.5
32670_at	*THBS3*	Thrombospondin 3	7059	2.3
31902_at	*DIO2*	Deiodinase, iodothyronine, type II	1734	3.3
38618_at	*LIMK2*	LIM domain kinase 2	3985	2.1
36686_at	*ALDH1A3*	Aldehyde dehydrogenase 1 family, member A3	220	2.3
36941_at	*MLLT11*	ALL1-fused gene from chromosome 1q	10962	7.2
32818_at	*TNC*	Hexabrachion (tenascin C, cytotactin)	3371	2.8
37147_at	*CLEC11A*	Stem cell growth factor; lymphocyte secreted C-type lectin	6320	2.2
38026_at	*FBLN1*	Fibulin 1	2192	2.1
32610_at	*PDLIM4*	PDZ and LIM domain 4	8572	2.7
2053_at	*CDH2*	Cadherin 2, type 1, N-cadherin (neuronal)	1000	3.0
35168_f_at	*COL16A1*	Collagen, type XVI, α1	1307	3.5

CA). All lysates were boiled in Laemmli buffer for 5 minutes before resolving by SDS-PAGE, and transferring onto nitrocellulose membranes. Equal loading onto polyacrylamide gels was confirmed by Ponceau S staining. Proteins were immunoblotted with the indicated primary antibodies, followed by incubation with horseradish peroxidase-conjugated secondary antibodies. Immunoblots were developed using enhanced chemiluminescence (Pierce, Rockford, IL).

Statistical Analysis

Data analysis of experiments using RLFs was performed using two-tailed Student's *t*-tests or one- or two-way analysis of variance, followed by Bonferroni post hoc testing. For experiments comparing categorical data, analysis was performed by creating contingency tables and applying χ^2 or Fisher's exact tests. All computations were performed with Microsoft Excel and GraphPad Prism software version 4.0c.

Results

Gene Expression Profiling Identifies Twist1 as the Most Consistently Up-Regulated Transcription Factor in IPF Lungs

IPF tissue samples were selected for presence of fibroblastic foci. Unsupervised clustering of gene expression data revealed two primary branches that corresponded to either IPF or control lungs (data not shown), indicating that IPF lungs exhibited a unique gene expression signature. Among the 30 most consistently up-regulated genes were several proteins previously associated with IPF, such as several extracellular matrix proteins and *IGFBP-5* (Table 1).[19] One of the most consistently up-regulated genes was *twist1* (Table 2 and Figure 1A). Interestingly, although earlier gene expression profiling studies of this disease did not identify *twist1* as being up-regulated,[20–22] a recent reanalysis of microarray data did identify *twist1* as being-up-regulated, although this result was not explored further.[23] Quantitative RT-PCR (qRT-PCR) confirmed these results (Figure 1B). Strong immunoreactivity against Twist1 protein was present in the nuclei of multiple cells types in IPF but not control lungs, particularly interstitial cells within fibroblastic foci as well as type II alveolar epithelial cells (Figure 1C).

Twist1 Is Induced by Profibrotic GFs and Promotes Fibroblast Accumulation and Survival

We found that several pro-fibrotic GFs associated with IPF, such as bFGF, PDGF, and EGF, all induced expression of Twist1 mRNA (Figure 2A) and protein (Figure 2, B and C) in primary RLFs. Other proteins that have been shown to induce Twist1 in other cell types, such as protein S,[13] tumor necrosis factor-α (TNF-α),[14] Wnt-1,[24] and

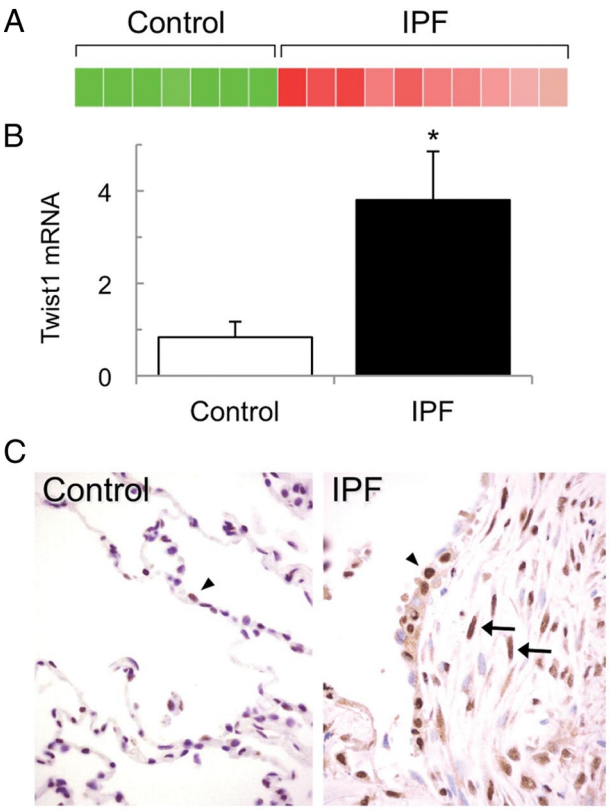

Figure 1. Expression of Twist1 in lungs from IPF patients. **A:** Heat map of Twist1 mRNA expression derived from microarray data. **B:** Quantitative RT-PCR of Twist mRNA normalized to glyceraldehyde-3-phosphate dehydrogenase mRNA obtained from lungs from IPF patients ($n = 7$) and controls ($n = 5$). Data represent mean ± SEM; $^{*}P < 0.05$. **C:** Immunohistochemistry of control and IPF lungs using affinity-purified IgG against Twist1. Twist1 was localized to the nuclei of fibroblasts (**arrows**) and type II epithelial cells (**arrowhead**) in a fibroblastic focus. Control lungs and isotype control staining demonstrated little detectable staining. Magnification, ×400.

insulin-like growth factor-I[25] were without effect, as were other profibrotic GFs, such as endothelin-1, Connective Tissue Growth Factor, and transforming growth factor-β (Figure 2A and data not shown). On the basis of the known biology of Twist1 in other cell types, we hypothesized that Twist1 expression promotes cell proliferation and/or cell viability in RLFs. We screened five siRNA oligonucleotides and identified two that consistently reduced expression of Twist1 mRNA and protein, although one was particularly potent (Figure 3, A–C). We noticed that the number of RLFs was reduced following transfection of Twist1 siRNA, but not control oligonucleotides (Figure 4, A and B). To distinguish between a requirement for Twist1 in cell proliferation and viability, we measured BrdU incorporation in RLFs transfected with Twist1 siRNA and found that knockdown of Twist1 had no effect on BrdU incorporation in cells (Figure 4C). In contrast, reduction of Twist1 expression by siRNA resulted in enhanced activity of caspase-3, a marker of apoptosis (Figure 4D).

Twist1 Protects against Apoptotic Stimuli Found in IPF Lungs

Various apoptotic stimuli are present in IPF lungs, including oxidants,[2] endoplasmic reticulum (ER) stress,[26,27] Fas ligand, and TNF-α.[28,29] Remarkably, fibroblasts in IPF lungs exhibit few signs of apoptosis.[2] We determined that the proapoptotic peroxidated lipid 4-HNE was present throughout IPF lungs, particularly in alveolar macrophages, and to a lesser extent, in type II alveolar epithelial cells, and fibroblasts/myofibroblasts (Supplemental Figure 1, see *http://ajp.amjpathol.org*). Overexpression of Twist1 led to increased viability of cells exposed to high concentrations of 4-HNE and the ER stress-inducing molecule thapsigargin (Figure 5A), whereas knockdown of Twist1 resulted in increased caspase-3 activity following addition of lower concentrations of these proapoptotic stimuli, and of Fas ligand and TNF-α (Figure 5B).

Bim and PUMA Mediate Apoptosis following Twist1 Knockdown

Because Twist1 expression was required for maximal cell viability even in the apparent absence of exogenous apoptotic stimuli (Figure 4), and several members of the BH3 family of proteins function in both the intrin-

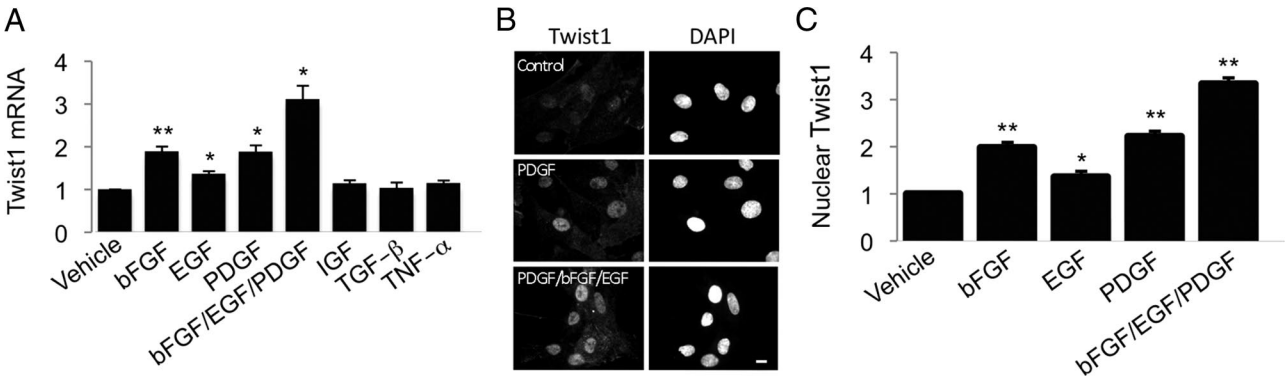

Figure 2. Expression of Twist1 in response to profibrotic GFs in primary RLFs. **A:** RLFs, maintained in 0.5% FBS, were incubated with 10 ng/ml of the indicated GFs for 16 hours at 37°C. RNA was isolated and subjected to qRT-PCR of Twist1 mRNA, normalized to PPIA mRNA. Data, expressed as fold increase over baseline, represent mean ± SEM, $n = 6–8$. $^{*}P < 0.05$; $^{**}P < 0.01$. **B:** Adherent RLFs were incubated with 10 ng/ml of the indicated GFs for 16 hours and processed for indirect immunofluorescence using affinity-purified rabbit IgG against Twist1 and DAPI. Bar = 10 μm. **C:** Twist1 nuclear staining fluorescence intensity was quantitated as described in *Materials and Methods*. Data represent mean ± SEM from >80 cells from at least three independent experiments. $^{*}P < 0.005$; $^{**}P < 0.001$.

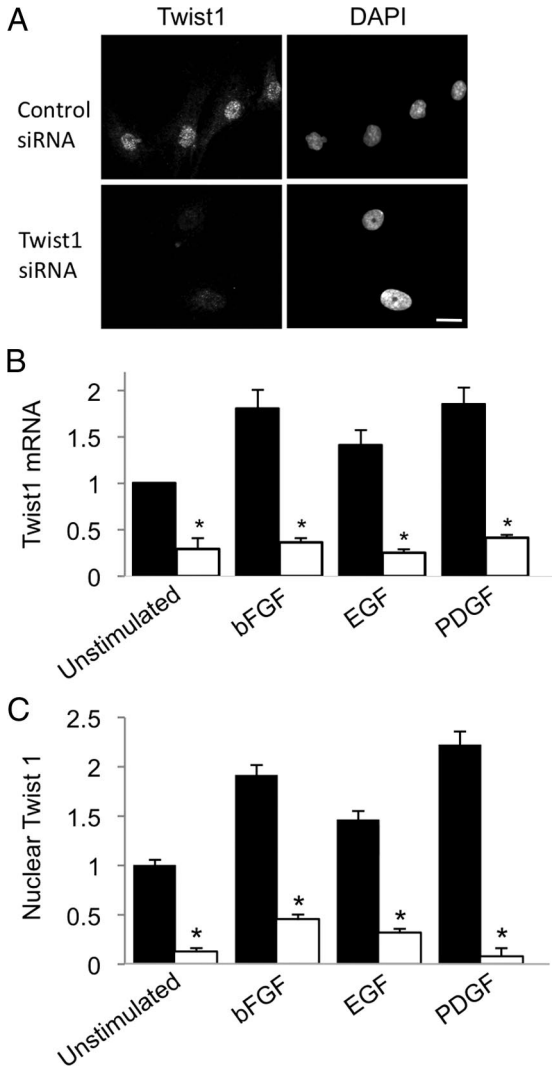

Figure 3. Reduction of Twist1 mRNA and protein in response to Twist1 siRNA. **A:** Adherent RLFs maintained in 0.5% FBS were incubated in the presence of either Twist1 or control siRNA oligonucleotides for 3 days at 37°C as described in *Materials and Methods* and processed for indirect immunofluorescence using affinity-purified rabbit IgG against Twist1 (**left panels**) and DAPI (**right panels**). Micrographs representative of at least 10 separate experiments. Bar = 10 μm. **B:** Adherent RLFs, incubated in the presence of either Twist1 (white bars) or control (black bars) siRNA oligonucleotides for 3 days at 37°C and in the presence or absence of the indicated growth factors for the last 24 hours. RNA was isolated and subjected to quantitative RT-PCR for Twist1 mRNA, normalized to PPIA mRNA. Data, expressed as fold-increase over baseline, represent mean ± SEM, $n = 6$; $^{*}P < 0.05$. **C:** Twist-1 nuclear staining fluorescence intensity was quantitated as described in *Materials and Methods*. Twist1 expression did not qualitatively differ between untransfected cells and cells transfected with scrambled control oligomers (data not shown). Data represent mean ± SEM from at least 100 cells from at least four independent experiments. $^{*}P < 0.001$.

sic or extrinsic apoptotic pathways,[30,31] we screened for changes in mRNA of these proteins following suppression of Twist1 with siRNA. We found that mRNA for Bim, PUMA, and Bik were increased when Twist1 was reduced (Figure 6A). As expected, Bim and PUMA protein were also up-regulated (Figure 6B), but we were unable to detect Bik induction by immunoblotting or immunofluorescence using three different anti-Bik antibodies (data not shown). We also detected slight decreases in the antiapoptotic proteins Bcl-2 and Mcl-1, but no changes in

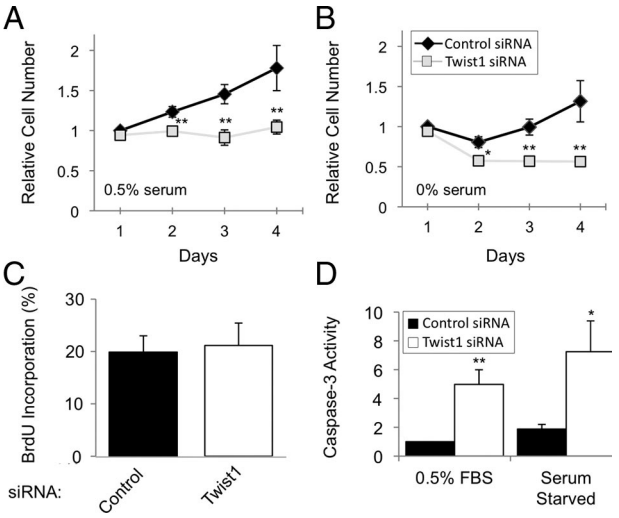

Figure 4. Effect of Twist1 siRNA on cell number, proliferation, and caspase-3 activity in RLFs. **A** and **B:** RLFs, transfected with the indicated siRNA oligonucleotides, were incubated as indicated and relative cell number was determined as described in *Materials and Methods*. Data represent mean ± SEM, $n = 6$; $^{*}P < 0.05$; $^{**}P < 0.005$. **C:** RLFs were incubated as in **A** and **B**, and 10 μmol/L BrdU was added for the final 18 hours before immunofluorescence using a mAb against BrdU. Data represent mean ± SEM, $n = 6$. **D:** RLFs were incubated as in **A** and **B**, and caspase-3 activity was measured as described in *Materials and Methods*. Data represent mean ± SEM, $n = 4$ (serum starved) or 11 (0.5% serum); $^{*}P < 0.05$; $^{**}P < 0.005$.

Bak, Bax, Bcl-X_L, and the active (nonphosphorylated) form of Bad (Figure 6B). The slight reduction in Bcl-2 expression is consistent with an earlier study,[32] but the lack of significant change of Bax expression was unexpected.[33] We then tested whether knockdown of Bim or

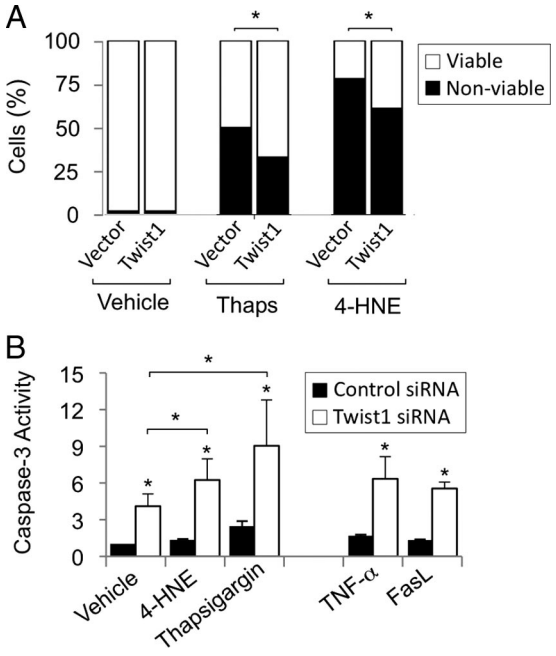

Figure 5. Effect of Twist1 overexpression on survival of RLFs challenged with proapoptotic factors present in fibrotic lungs. **A:** RLFs transfected with FLAG-tagged Twist1 were exposed to oxidant (12 μmol/L 4-HNE) and ER stress (2 μmol/L thapsigargin; (Thaps)) in the presence of 0.5% FBS overnight. Cell number was quantified as described in *Materials and Methods* ($n = 4595$ cells analyzed); $^{*}P < 0.01$. **B:** Two days after transfection with Twist siRNA, RLFs were stimulated with apoptosis-inducing stimuli (5 μmol/L 4-HNE, 0.8 μmol/L thapsigargin, 50 ng/ml TNF-α, or 10 ng/ml Fas ligand (FasL)) in 0.5% FBS. Apoptosis was measured by caspase-3 activity and normalized to cell number. Data represent mean ± SEM, $n = 4$. $^{*}P < 0.05$.

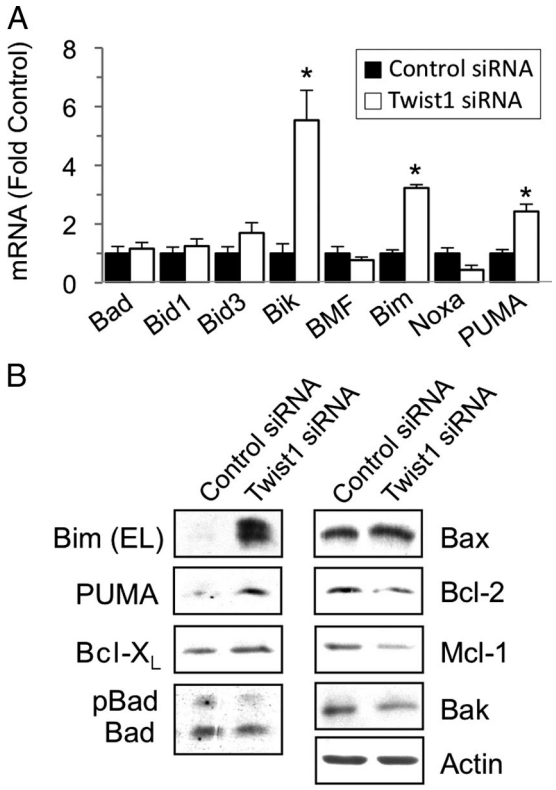

Figure 6. Effect of Twist1 siRNA on expression of Bcl-2 family members. **A:** RLFs were incubated with Twist1 (white bars) or control (black bars) siRNA, and RNA was extracted and processed for qRT-PCR of the indicated BH3-only family members normalized to PPIA mRNA. Data represent mean ± SEM, $n = 3$–5. $^{*}P < 0.001$. **B:** RLFs were incubated with siRNA oligonucleotides as described in **A**, and detergent extracts were prepared and subjected to SDS-PAGE and immunoblotting using the indicated antibodies. Data are representative of three independent experiments.

PUMA influenced the sensitivity of RLFs to apoptosis mediated by Twist1 reduction. Transfection of shRNA constructs against Bim and PUMA, but not control shRNA, resulted in decreased expression of these proteins (Supplemental Figure 2, A and B, see *http://ajp.amjpathol.org*). Subsequent transfection of Twist1 siRNA increased the fraction of nonviable cells expressing control shRNA from 9 to 22%, but to only 12% in cells lacking Bim and 16% in cells lacking PUMA (Figure 7, A and B), indicating that Bim and PUMA contributed to apoptosis following Twist1 depletion. Cotransfection of both shRNA plasmids simultaneously resulted in inefficient knockdown of both proteins (data not shown).

PDGF Induces Apoptosis in RLFs Lacking Twist1

We transfected RLFs with Twist1 siRNA oligomers and stimulated the cells with various GFs for the last 18 hours. Knockdown of Twist1 resulted in fewer cells, regardless of the cell culture conditions (Figure 8, A and B). As expected, addition of either bFGF or EGF mitigated this effect, but to our surprise, addition of PDGF was incapable of doing so (Figure 8, A and B), despite the fact that this growth factor was, if anything, a more potent mitogen for these cells. Even more striking, addition of all three GFs together sensitized RLFs to the loss of cells in response to decreased Twist1 expression, although the proliferative response to these mitogens was preserved (Figure 8C). PDGF, and particularly all three GFs to-

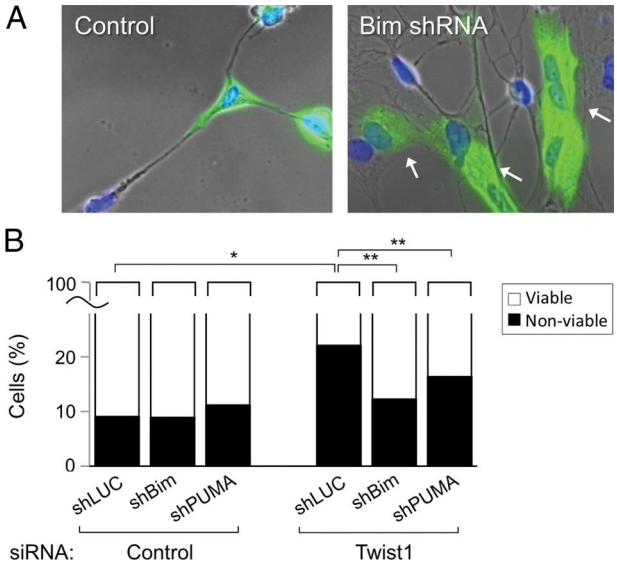

Figure 7. Effects of shRNA-based reduction in Bim and PUMA expression on Twist1 siRNA-induced cell death. **A:** RLFs were cotransfected with the indicated shRNA-encoding plasmids and a plasmid encoding EGFP, replated in the presence of Twist siRNA oligonucleotides on the following day, and incubated in 0.5% serum for an additional 72 hours at 37°C. Cells were fixed, stained with DAPI, and visualized by fluorescence microscopy. Note small condensed nuclei typical of late-stage apoptosis, in cells expressing control shRNA (**left panel**) or EGFP-negative cells not expressing Bim shRNA (**right panel**). Preservation of nuclear morphology was apparent in cells expressing EGFP- and Bim shRNA-encoding plasmid (**arrows**). **B:** EGFP-expressing cells were scored for the presence or absence of apoptotic nuclei. Bars represent total cells counted, $n = 800$–2000 cells from eight separate experiments. $^{*}P < 0.01$; $^{**}P < 0.001$.

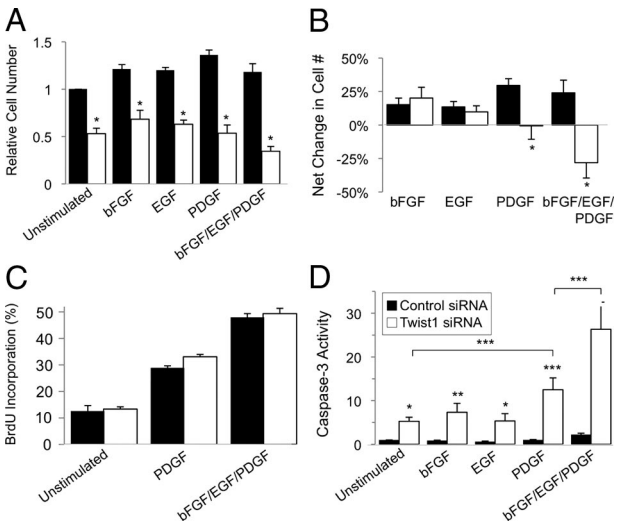

Figure 8. Effect of Twist1 knockdown on cell survival in the presence of pro-fibrotic GFs. **A**, **B:** Two days after transfection with either control (white bars) or Twist1 (black bars) siRNA, RLFs were incubated with 10 ng/ml of the indicated GFs overnight in 0.5% FBS, and relative cell number was quantitated as described in *Materials and Methods*. The number of growth factor stimulated cells was compared with unstimulated cells on day 3. Note that cell number was unchanged by PDGF and was decreased by bFGF, EGF, and PDGF in cells transfected with Twist1 (white bars) but not control (black bars) siRNA. Data represent mean ± SEM, $n = 4$. $^{*}P < 0.05$. **C**, **D:** RLFs were incubated as in **A** and BrdU incorporation (**C**) and caspase-3 activity (**D**) was measured as described in *Materials and Methods*. Data represent mean ± SEM, $n = 4$–7. $^{*}P < 0.02$; $^{**}P < 0.002$; $^{***}P < 0.0001$.

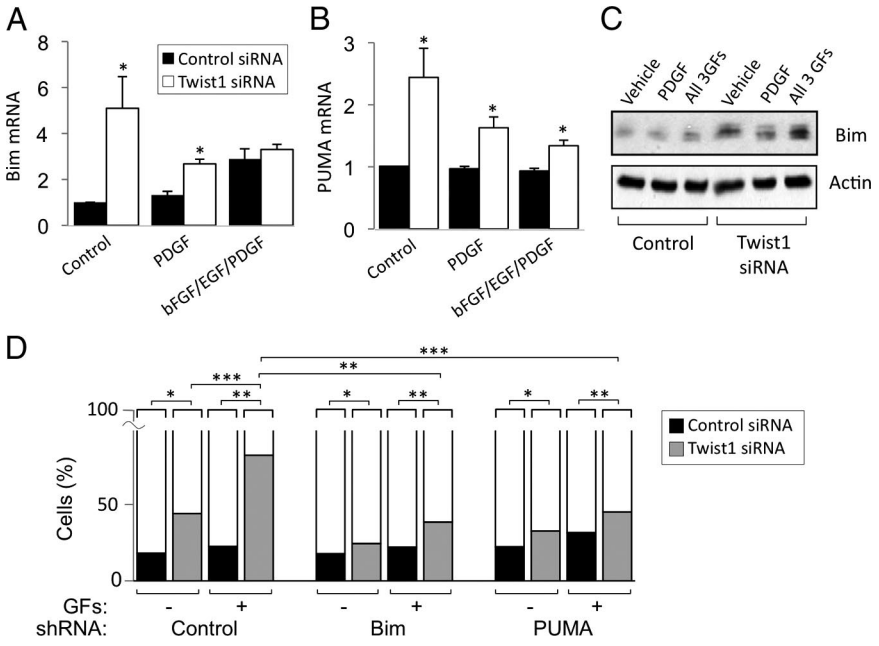

Figure 9. Effects of shRNA-based reduction in Bim and PUMA expression on cell death induced by Twist1 siRNA and GFs. **A** and **B:** RLFs were incubated with Twist1 (white bars) or control (black bars) siRNA and 10 ng/ml PDGF or a combination of 10 ng/ml each bFGF, EGF, and PDGF were added for the final 24 hours. RNA was extracted and processed for qRT-PCR of Bim (**A**) or PUMA (**B**) normalized to PPIA expression. Data represent mean ± SEM, $n = 4$. $^{*}P < 0.001$. **C:** Immunoblot of RLF lysates treated as described in **A** and **B**. **D:** RLFs were cotransfected with a plasmid encoding EGFP and the indicated shRNA-encoding plasmids and replated in the presence of Twist siRNA oligonucleotides in 0.5% serum for 3 days. In the last 24 hours, cells were incubated in the presence of 10 ng/ml each of bFGF, EGF, and PDGF. Fixed cells were stained with DAPI, and EGFP-expressing cells were scored for the presence or absence of apoptotic nuclei. White bars, viable cells; grey or black bars, nonviable cells. Data represent mean ± SEM, $n = 200–600$ cells from three to five separate experiments. $^{*}P < 0.01$; $^{**}P < 0.001$; $^{***}P < 0.0001$.

gether, caused enhanced caspase-3 activity in cells lacking Twist1 (Figure 8D), indicating that the accelerated loss of cell numbers induced by the GFs was due to increased apoptosis, rather than decreased proliferation. This was accompanied by increased expression of Bim mRNA (Figure 9A) and protein (Figure 9C) but not PUMA (Figure 9B and data not shown). Bim expression was greatest in GF-treated cells transfected with Twist1 siRNA oligonucleotides (Figure 9C). Interestingly, addition of GFs in the absence of Twist1 reduction led to slight increase in Bim expression (Figure 9, A and C). When we examined the viability of cells expressing either shBim or shPUMA during Twist1 knockdown and GF stimulation, we found that PUMA and particularly Bim shRNA reduced the extent of apoptosis following Twist1 knockdown in the presence of GFs (Figure 9D). Overexpression of Twist1 led to decreased Bim expression in RLFs exposed to high concentrations of 4-HNE and the ER stress-inducing molecule thapsigargin (Figure 10).

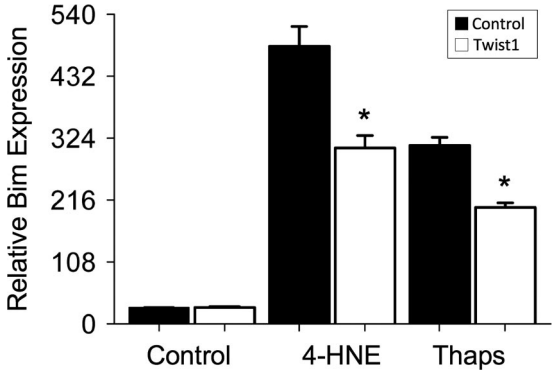

Figure 10. Effect of Twist1 overexpression on Bim expression. RLFs transfected with FLAG-tagged Twist1 (white bars) or control plasmids (black bars) were exposed to oxidant (12 μmol/L 4-HNE) or ER stress (2 μmol/L thapsigargin; (Thaps)) in the presence of 0.5% FBS overnight. Cell number was quantified as described in *Materials and Methods* ($n = 250$ cells/condition analyzed); $^{*}P < 0.0001$.

Discussion

Numerous studies have failed to detect apoptosis in fibroblasts in IPF lungs, suggesting that resistance to cell death may contribute to the persistence of fibroblasts and the pathogenesis of IPF. Although multiple proapoptotic factors have been identified in IPF lungs, such is not the case for antiapoptotic factors. Here, we identified Twist1 as a highly up-regulated gene in the lungs of patients with IPF. Using a variety of approaches, we demonstrated the capacity of Twist1 to protect RLFs from apoptosis *in vitro*. Apoptosis in RLFs following suppression of Twist1 was mediated, in part, by up-regulation of Bim and PUMA. Finally, profibrotic GFs induced Twist1 expression in RLFs, which was necessary to protect these cells from apoptosis, particularly in the continued presence of these GFs. We suggest that Twist1 promotes fibroblast viability by ensuring that cells exposed simultaneously to GFs and proapoptotic stimuli preferentially exhibit a survival phenotype. In this respect, Twist1-expressing primary lung fibroblasts behave much like Twist1 overexpressing neoplastic cells treated with chemotherapeutic agents[16,18] and other apoptotic stimuli.[15]

Basic FGF, EGF, and PDGF may all contribute to the pathogenesis of IPF[34–36] and are mitogens for fibroblasts. Depletion of Twist1 in RLFs did not abrogate the mitogenic response to these GFs, although fibroblast accumulation was impaired due to the overriding effect of Twist1 depletion on apoptosis. It was striking and unexpected that PDGF, particularly in conjunction with other GFs, appeared to act as an apoptotic stimulus when Twist1 expression was reduced with siRNA. Although GFs are typically thought of as promoting survival, PDGF has been shown to induce apoptosis in confluent vascular smooth muscle cells[37] and serum-deprived kidney fibroblasts, which intriguingly, was potentiated by EGF.[38]

What factors govern the sensitivity of RLFs to GF-induced apoptosis? We suggest that Twist1 is one such factor as its expression is critical for shaping the response of fibroblasts to the combined effects of pro-growth and proapoptotic factors. The need for such a function is underscored by the fact that PDGF and other GFs signal through myc and p38, both of which have the dual capacity to promote proliferation[39,40] as well as apoptosis.[41,42] We speculate that Twist1 expression may be critical to inhibit apoptosis but not other downstream pathways of myc and/or p38, thereby providing a counterbalancing force necessary for survival. Thus, Twist1 may uncouple proliferative from apoptotic signaling downstream of GFs.

We found that expression of Bim and PUMA was increased when Twist1 was knocked down in unstimulated cells, and both proteins partially mediated apoptosis under these conditions. In addition, mRNA for the BH3-only protein Bik was induced, but we were unable to detect Bik protein using three different antibodies. This may have been because Bik was below the limit of detection of our antibodies or rapidly degraded by the proteasome.[43] Several potential Twist1 targets have been shown to up-regulate Bim and PUMA, including c-Jun N-terminal kinase,[44] FoxO,[45,46] and p53.[47,48] In preliminary experiments, we were unable to detect c-Jun N-terminal kinase activation following Twist1 knockdown, and we did not find evidence of increased accumulation of nuclear FoxO proteins or of the unphosphorylated transcriptionally active forms (data not shown). Twist1 prevents activation of p53 through multiple mechanisms, such as down-regulation of alternative reading frame protein (ARF),[15] and through direct interactions.[49] Further experiments will be necessary to determine what role p53 plays in RLFs following Twist1 depletion.

In the context of its antiapoptotic function, does Twist1 act as a transcriptional activator, a transcriptional repressor, or perhaps neither? In addition to p53, Twist1 interacts with a number of other transcription factors, including p65 nuclear factor κB[14] and Runx2.[11] The C terminus of Twist1 directly binds and inhibits p65 nuclear factor κB, and this interaction represses production of the proapoptotic cytokine, TNF-α.[14] Interestingly, TNF-α may promote fibrosis, in part, by promoting epithelial cell apoptosis, suggesting another possible role for Twist1 in these cells. However, as nuclear factor κB is generally antiapoptotic in fibroblasts,[50] Twist1 may be acting by additional means in these cells. The Twist1 C terminus also binds to Runx2, thereby inhibiting Runx2-dependent transcription. Interestingly, Runx3 is a known tumor suppressor that induces apoptosis, in part, by up-regulating Bim.[51]

Twist1 was present in other cell types present in IPF lungs, and it is possible that Twist1 exerts profibrotic effects in multiple cell populations. Twist1 has been implicated in EMT in various cancers,[17,52] and several groups have presented evidence that EMT contributes to IPF.[6,7] A deeper understanding of Twist1 function in fibrosis will require a suitable animal model of fibrosis, such as a transgenic mouse model in which Twist1 biological activity is regulated in a tissue-specific and inducible fashion.

References

1. Meltzer EB, Noble PW: Idiopathic pulmonary fibrosis. Orphanet J Rare Dis 2008, 3:8
2. Thannickal VJ, Horowitz JC: Evolving concepts of apoptosis in idiopathic pulmonary fibrosis. Proc Am Thorac Soc 2006, 3:350–356
3. Phillips RJ, Burdick MD, Hong K, Lutz MA, Murray LA, Xue YY, Belperio JA, Keane MP, Strieter RM: Circulating fibrocytes traffic to the lungs in response to CXCL12 and mediate fibrosis. J Clin Invest 2004, 114:438–446
4. Andersson-Sjoland A, de Alba CG, Nihlberg K, Becerril C, Ramirez R, Pardo A, Westergren-Thorsson G, Selman M: Fibrocytes are a potential source of lung fibroblasts in idiopathic pulmonary fibrosis. Int J Biochem Cell Biol 2008, 40:2129–2140
5. Hashimoto N, Jin H, Liu T, Chensue SW, Phan SH: Bone marrow-derived progenitor cells in pulmonary fibrosis. J Clin Invest 2004, 113:243–252
6. Kim KK, Kugler MC, Wolters PJ, Robillard L, Galvez MG, Brumwell AN, Sheppard D, Chapman HA: Alveolar epithelial cell mesenchymal transition develops in vivo during pulmonary fibrosis and is regulated by the extracellular matrix. Proc Natl Acad Sci USA 2006, 103: 13180–13185
7. Willis BC, Liebler JM, Luby-Phelps K, Nicholson AG, Crandall ED, du Bois RM, Borok Z: Induction of epithelial-mesenchymal transition in alveolar epithelial cells by transforming growth factor-β1: potential role in idiopathic pulmonary fibrosis. Am J Pathol 2005, 166:1321–1332
8. Kass D, Bridges RS, Borczuk A, Greenberg S: Methionine aminopeptidase-2 as a selective target of myofibroblasts in pulmonary fibrosis. Am J Respir Cell Mol Biol 2007, 37:193–201
9. Selman M, Ruiz V, Cabrera S, Segura L, Ramirez R, Barrios R, Pardo A: TIMP-1, -2, -3, and -4 in idiopathic pulmonary fibrosis: a prevailing nondegradative lung microenvironment? Am J Physiol 2000, 279: L562–L574
10. Uhal BD, Joshi I, Hughes WF, Ramos C, Pardo A, Selman M: Alveolar epithelial cell death adjacent to underlying myofibroblasts in advanced fibrotic human lung. Am J Physiol Lung Cell Mol Physiol 1998, 275:L1192–L1199
11. Bialek P, Kern B, Yang X, Schrock M, Sosic D, Hong N, Wu H, Yu K, Ornitz DM, Olson EN, Justice MJ, Karsenty G: A twist code determines the onset of osteoblast differentiation. Dev Cell 2004, 6:423–435
12. Rice DP, Aberg T, Chan Y, Tang Z, Kettunen PJ, Pakarinen L, Maxson RE, Thesleff I: Integration of FGF and TWIST in calvarial bone and suture development. Development 2000, 127:1845–1855
13. Sharif MN, Sosic D, Rothlin CV, Kelly E, Lemke G, Olson EN, Ivashkiv LB: Twist mediates suppression of inflammation by type I IFNs and Axl. J Exp Med 2006, 203:1891–1901
14. Sosic D, Richardson JA, Yu K, Ornitz DM, Olson EN: Twist regulates cytokine gene expression through a negative feedback loop that represses NF-κB activity. Cell 2003, 112:169–180
15. Maestro R, Dei Tos AP, Hamamori Y, Krasnokutsky S, Sartorelli V, Kedes L, Doglioni C, Beach DH, Hannon GJ: Twist is a potential oncogene that inhibits apoptosis. Genes Dev 1999, 13:2207–2217
16. Cheng GZ, Chan J, Wang Q, Zhang W, Sun CD, Wang LH: Twist transcriptionally up-regulates AKT2 in breast cancer cells leading to increased migration, invasion, and resistance to paclitaxel. Cancer Res 2007, 67:1979–1987
17. Yang J, Mani SA, Donaher JL, Ramaswamy S, Itzykson RA, Come C, Savagner P, Gitelman I, Richardson A, Weinberg RA: Twist, a master regulator of morphogenesis, plays an essential role in tumor metastasis. Cell 2004, 117:927–939
18. Wang X, Ling MT, Guan XY, Tsao SW, Cheung HW, Lee DT, Wong YC: Identification of a novel function of TWIST, a bHLH protein, in the development of acquired Taxol resistance in human cancer cells. Oncogene 2004, 23:474–482
19. Pilewski JM, Liu L, Henry AC, Knauer AV, Feghali-Bostwick CA: Insulin-like growth factor binding proteins 3 and 5 are overexpressed in idiopathic pulmonary fibrosis and contribute to extracellular matrix deposition. Am J Pathol 2005, 166:399–407
20. Pardo A, Gibson K, Cisneros J, Richards TJ, Yang Y, Becerril C,

Yousem S, Herrera I, Ruiz V, Selman M, Kaminski N: Up-regulation and profibrotic role of osteopontin in human idiopathic pulmonary fibrosis. PLoS Med 2005, 2:e251
21. Zuo F, Kaminski N, Eugui E, Allard J, Yakhini Z, Ben-Dor A, Lollini L, Morris D, Kim Y, DeLustro B, Sheppard D, Pardo A, Selman M, Heller RA: Gene expression analysis reveals matrilysin as a key regulator of pulmonary fibrosis in mice and humans. Proc Natl Acad Sci USA 2002, 99:6292–6297
22. Yang IV, Burch LH, Steele MP, Savov JD, Hollingsworth JW, McElvania-Tekippe E, Berman KG, Speer MC, Sporn TA, Brown KK, Schwarz MI, Schwartz DA: Gene expression profiling of familial and sporadic interstitial pneumonia. Am J Respir Crit Care Med 2007, 175:45–54
23. Selman M, Pardo A, Kaminski N: Idiopathic pulmonary fibrosis: aberrant recapitulation of developmental programs? PLoS Med 2008, 5:e62
24. Howe LR, Watanabe O, Leonard J, Brown AM: Twist is up-regulated in response to Wnt1 and inhibits mouse mammary cell differentiation. Cancer Res 2003, 63:1906–1913
25. Dupont J, Fernandez AM, Glackin CA, Helman L, LeRoith D: Insulin-like growth factor 1 (IGF-1)-induced twist expression is involved in the anti-apoptotic effects of the IGF-1 receptor. J Biol Chem 2001, 276:26699–26707
26. Korfei M, Ruppert C, Mahavadi P, Henneke I, Markart P, Koch M, Lang G, Fink L, Bohle RM, Seeger W, Weaver TE, Guenther A: Epithelial Endoplasmic Reticulum stress and apoptosis in sporadic Idiopathic Pulmonary Fibrosis, Am J Respir Crit Care Med 2008, 178:838–846
27. Lawson WE, Crossno PF, Polosukhin VV, Roldan J, Cheng DS, Lane KB, Blackwell TR, Xu C, Markin C, Ware LB, Miller GG, Loyd JE, Blackwell TS: Endoplasmic reticulum stress in alveolar epithelial cells is prominent in IPF: association with altered surfactant protein processing and herpesvirus infection. Am J Physiol Lung Cell Mol Physiol 2008, 294:L1119–L1126
28. Kuwano K, Kawasaki M, Maeyama T, Hagimoto N, Nakamura N, Shirakawa K, Hara N: Soluble form of fas and fas ligand in BAL fluid from patients with pulmonary fibrosis and bronchiolitis obliterans organizing pneumonia. Chest 2000, 118:451–458
29. Ziegenhagen MW, Schrum S, Zissel G, Zipfel PF, Schlaak M, Muller-Quernheim J: Increased expression of proinflammatory chemokines in bronchoalveolar lavage cells of patients with progressing idiopathic pulmonary fibrosis and sarcoidosis. J Invest Med 1998, 46:223–231
30. Han J, Goldstein LA, Gastman BR, Rabinowich H: Interrelated roles for Mcl-1 and BIM in regulation of TRAIL-mediated mitochondrial apoptosis. J Biol Chem 2006, 281:10153–10163
31. Huang S, Sinicrope FA: BH3 mimetic ABT-737 potentiates TRAIL-mediated apoptotic signaling by unsequestering Bim and Bak in human pancreatic cancer cells. Cancer Res 2008, 68:2944–2951
32. Pham CG, Bubici C, Zazzeroni F, Knabb JR, Papa S, Kuntzen C, Franzoso G: Up-regulation of Twist-1 by NF-κB blocks cytotoxicity induced by chemotherapeutic drugs. Mol Cell Biol 2007, 27:3920–3935
33. Kwok WK, Ling MT, Lee TW, Lau TC, Zhou C, Zhang X, Chua CW, Chan KW, Chan FL, Glackin C, Wong YC, Wang X: Up-regulation of TWIST in prostate cancer and its implication as a therapeutic target. Cancer Res 2005, 65:5153–5162
34. Inoue Y, King TE, Jr., Barker E, Daniloff E, Newman LS: Basic fibroblast growth factor and its receptors in idiopathic pulmonary fibrosis and lymphangioleiomyomatosis. Am J Respir Crit Care Med 2002, 166:765–773
35. Ishii Y, Fujimoto S, Fukuda T: Gefitinib prevents bleomycin-induced lung fibrosis in mice. Am J Respir Crit Care Med 2006, 174:550–556
36. Bonner JC: Regulation of PDGF and its receptors in fibrotic diseases. Cytokine Growth Factor Rev 2004, 15:255–273
37. Okura T, Igase M, Kitami Y, Fukuoka T, Maguchi M, Kohara K, Hiwada K: Platelet-derived growth factor induces apoptosis in vascular smooth muscle cells: roles of the Bcl-2 family. Biochim Biophys Acta 1998, 1403:245–253
38. Kim HR, Upadhyay S, Li G, Palmer KC, Deuel TF: Platelet-derived growth factor induces apoptosis in growth-arrested murine fibroblasts. Proc Natl Acad Sci USA 1995, 92:9500–9504
39. Armelin HA, Armelin MC, Kelly K, Stewart T, Leder P, Cochran BH, Stiles CD: Functional role for c-myc in mitogenic response to platelet-derived growth factor. Nature 1984, 310:655–660
40. Yamaguchi H, Igarashi M, Hirata A, Susa S, Ohnuma H, Tominaga M, Daimon M, Kato T: Platelet-derived growth factor BB-induced p38 mitogen-activated protein kinase activation causes cell growth, but not apoptosis, in vascular smooth muscle cells. Endocr J 2001, 48:433–442
41. Desbarats L, Schneider A, Muller D, Burgin A, Eilers M: Myc: a single gene controls both proliferation and apoptosis in mammalian cells. Experientia 1996, 52:1123–1129
42. Xia Z, Dickens M, Raingeaud J, Davis RJ, Greenberg ME: Opposing effects of ERK and JNK-p38 MAP kinases on apoptosis. Science 1995, 270:1326–1331
43. Hur J, Bell DW, Dean KL, Coser KR, Hilario PC, Okimoto RA, Tobey EM, Smith SL, Isselbacher KJ, Shioda T: Regulation of expression of BIK proapoptotic protein in human breast cancer cells: p53-dependent induction of BIK mRNA by fulvestrant and proteasomal degradation of BIK protein. Cancer Res 2006, 66:10153–10161
44. Wong HK, Fricker M, Wyttenbach A, Villunger A, Michalak EM, Strasser A, Tolkovsky AM: Mutually exclusive subsets of BH3-only proteins are activated by the p53 and c-Jun N-terminal kinase/c-Jun signaling pathways during cortical neuron apoptosis induced by arsenite. Mol Cell Biol 2005, 25:8732–8747
45. Dijkers PF, Medema RH, Pals C, Banerji L, Thomas NS, Lam EW, Burgering BM, Raaijmakers JA, Lammers JW, Koenderman L, Coffer PJ: Forkhead transcription factor FKHR-L1 modulates cytokine-dependent transcriptional regulation of $p27^{KIP1}$. Mol Cell Biol 2000, 20:9138–9148
46. You H, Pellegrini M, Tsuchihara K, Yamamoto K, Hacker G, Erlacher M, Villunger A, Mak TW: FOXO3a-dependent regulation of Puma in response to cytokine/growth factor withdrawal. J Exp Med 2006, 203:1657–1663
47. Burns TF, El-Deiry WS: Microarray analysis of p53 target gene expression patterns in the spleen and thymus in response to ionizing radiation. Cancer Biol Ther 2003, 2:431–443
48. Nakano K, Vousden KH: PUMA, a novel proapoptotic gene, is induced by p53. Mol Cell 2001, 7:683–694
49. Shiota M, Izumi H, Onitsuka T, Miyamoto N, Kashiwagi E, Kidani A, Hirano G, Takahashi M, Naito S, Kohno K: Twist and p53 reciprocally regulate target genes via direct interaction. Oncogene 2008, DOI: 10.1038/onc.2008.176
50. Sarkar FH, Li Y: NF-κB: a potential target for cancer chemoprevention and therapy. Front Biosci 2008, 13:2950–2959
51. Yano T, Ito K, Fukamachi H, Chi XZ, Wee HJ, Inoue K, Ida H, Bouillet P, Strasser A, Bae SC, Ito Y: The RUNX3 tumor suppressor up-regulates Bim in gastric epithelial cells undergoing transforming growth factor β-induced apoptosis. Mol Cell Biol 2006, 26:4474–4488
52. Yang MH, Wu MZ, Chiou SH, Chen PM, Chang SY, Liu CJ, Teng SC, Wu KJ: Direct regulation of TWIST by HIF-1α promotes metastasis. Nat Cell Biol 2008, 10:295–305